RECENT ACHIEVEMENTS IN CHARACTERISING THE MAGNETOSPHERE, IONOSPHERE AND THERMOSPHERE

H. Lühr[1], S. Maus[2], C. Stolle[1], H. Liu[3] and M. Rother[1]

1) GFZ Potsdam, Telegrafenberg, D-14473 Potsdam, Germany, Email: hluehr@gfz-potsdam.de
2) Cooperative Inst. for Research in Environm. Sci., UC, Boulder, CO
3) Earth and Planetary Science Division, Hokkaido University, Japan

ABSTRACT

The recent magnetic field missions have brought about an enormous progress in the understanding of the near-Earth external field structure and the description of its sources. Furthermore, it has become clear that the geomagnetic field influences significantly the dynamics of the neutral particles in the upper atmosphere.

In the past, insufficient corrections of the external field contributions have often been the most limiting factor for the accuracy of geomagnetic field models. For an elimination of the magnetospheric contribution suitable models of the current systems are needed, which have to be adequately parameterised to account for the varying activity. Modelling these currents in appropriate coordinate systems (GSM, SM) and considering properly the induction effect make the correction much more effective.

The ionospheric influence on main field studies was assumed to be minimised by selecting data from quiet nights. More and more evidence has, however, been presented in recent years that sizable currents flow in the ionospheric F region even at night. These are driven predominantly by plasma processes. Here we show the effects of the diamagnetic effect, gravity driven currents and induced currents. A proposal for modelling them is outlined.

In the thermosphere neutral and charged particles are coexisting. Here thermodynamics and electrodynamics are controlling the motion of the particles. CHAMP, equipped with both an accelerator and a magnetometer, could determine for the first time, how strong the geomagnetic field is influencing the upper atmosphere. This forcing of the neutral particles can be observed both in the density distribution and in the wind field.

1. INTRODUCTION

It is generally accepted that the upper spheres of the Earth, magnetosphere, ionosphere and thermosphere form a highly coupled system. Studying their interactions is of great interest for the space science community. In this article we will, however, concentrate on the interaction of these spheres with the near-Earth magnetic field. In now-a-days geomagnetic field modeling the resolution of the instruments and the spatial coverage are no longer the limiting factors. It is more the proppper consideration of the field contributions coming from outside the Earth that is determining the quality of the derived models. During recent years a lot of progress could be made in better characterizing the external fields. Here we will point out the major achievements. The sources for external fields are conveniently divided in three groups, the magnetospheric currents well above the satellite, the ionospheric currents below the orbit and the field-aligned currents which couple both systems and which cross the satellite orbit (e.g. Langel et al., 1996). During pre-CHAMP times the following assumptions were made:

1) Magnetospheric field contributions are well ordered in dipole coordinates. Their amplitudes scale with D_{ST}.
2) Ionospheric currents at middle latitudes are negligible at night times.
3) All ionospheric currents are confined to the E-layer (90 – 150 km) except for field-aligned currents.

In the subsequent chapters we will show which of these assumptions are still valid and what are the consequences of the new findings. The last section will deal with the influence of the geomagnetic field on the thermosphere. This newly observed magnetic fingerprint even in the neutral gas dynamics underlines the high degree of coupling between the upper spheres.

2. MAGNETOSPHERIC FIELDS

Within the magnetosphere and on its boundaries a variety of different currents is flowing. Near the Earth surface only the effect of the large scale currents are sensed. Therefore the observed fields are rather homogeneous. The three prominent systems are the ring current, the magnetopause current and the magneto-tail current. In the past, all three of them have been modelled in dipole coordinates and the amplitude was scaled by the D_{ST} index (e.g. Olsen, 2002). This approach worked reasonably well for main field modelling where only night side data are considered. For refinements, later an additional term was introduced describing annual and semi-annual variations of the external field.

On the dayside, however, all these representations predicted the actual distribution of magnetospheric field rather poorly. The studies on ionospheric currents were badly affected by that short coming.

In a first attempt to improve this situation Maus et al. (2005) have started to model the near-Earth magnetic field in coordinates in which the current are best ordered. These are, in particular, the Geocentric-Solar-Magnetospheric (GSM) and the Solar- Magnetic (SM) frames. Currents in the outer magnetosphere, e.g. geomagnetic tail, which are directly influenced by the interaction of the solar wind with the geomagnetic field, should be described in GSM coordinates. Those currents closer to the Earth, e.g. ring currents, which are primarily controlled by the geometry of the geomagnetic field, are best ordered in SM coordinates. A refinement of this approach was presented by Maus and Lühr (2005) which includes a dedicated treatment of the induction effects associated with these magnetospheric fields.

A major component in this decomposition is a steady field of about 13 nT, pointing due south in the GSM frame. Due to the wobble of the geomagnetic dipole in the GSM frame diurnal and annual variations are observed at the Earth's surface. Figures 1a and b show the predicted variations in the three components for the location of the observatory Niemegk (NGK) over one year and one day, respectively. On top of the constant values there are diurnal variations which are amplitude modulated over a year. The diurnal variation for summer solstice is shown in Figure 1b. It is interesting to note that this signal is well in phase with the S_q variation. When looking at the winter solstice we find a diurnal signal which is in anti-phase with S_q. Thus, all the previous studies of the S_q field distribution are affected by not taking into account the GSM-related magnetospheric field.

When limiting the attention to an observatory reading at night time the GSM field will cause an annual variation of the components. Such variations have earlier been observed and were termed seasonal variation of observatory baseline (Campbell, 1984). The good agreement shown in Maus and Lühr (2005) between night time observatory data and their predicted external field for five different latitudes provides convincing evidence for the derived model. The same approach of decomposing the magnetospheric field into a SM and GSM part has also successfully been applied by Olsen et al. (2005a) when deriving their candidate model of the IGRF 2005.

The part of the magnetospheric field modelled in SM is attributed to the effect caused by the ring currents. Its amplitude follows the storm-time index, D_{ST}. Traditionally, the effect observed on the ground was attributed to originate partly from space (73%) and

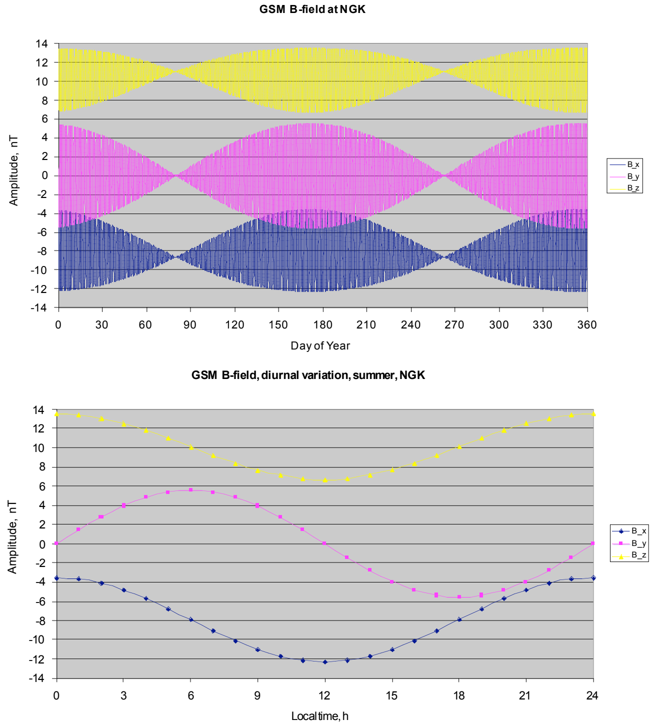

Figure 1. Signature of the stable GSM magnetic field at the location of Niemegk (NGK). (top panel) Due to the wobble of the geomagnetic dipole there is an annual and diurnal variation observed on ground. (bottom panel) The diurnal variation at June solstice resembles that of the Sq system. The magnetic field in GSM is believed to originate from the magnetospheric tail.

partly from the induction effect (27%) (Langel and Estes, 1985). It was pointed out by Maus and Weidelt (2004) that the induction effect is not represented well by this simple linear relation. They propose a decomposition of the index D_{ST} into E_{ST} and I_{ST} for the external and internal contributions of the ring current, respectively. The I_{ST} value is calculated based on a Q-response function derived from a representative 1-D conductivity model of the mantle (Utada et al., 2003) Maus and Weidelt (2004) showed that there are differences of ±5 nT between the fields derived by the traditional and new method. The differences build up during magnetic storms, but their decay takes several months. A detailed discussion of the frequency dependence of the induced part is also given by Olsen et al. (2005a).

In summary, the separate modelling of the magnetospheric field components in SM and in GSM coordinates allows for a much simpler characterisation of the sources during magnetically quiet times. Furthermore, the decomposition of the D_{ST} index into E_{ST} and I_{ST} provides a better representation of the ring current effect at off-equator latitudes. Taking both modifications together provides a much better description of the magnetospheric field, which will be favourable for main field modelling but also for ionospheric current studies on the dayside.

3. IONOSPHERIC FIELDS

Magnetic fields caused by ionospheric currents are particularly strong at auroral latitudes. These regions are, however, not considered here. Significant currents can also be found at mid and low latitudes on the dayside. On the night side the currents are much weaker since the conductivity in the ionospheric E region is reduced by about two orders of magnitude. For this reason models of the main geomagnetic field are derived from night time data. Traditionally, a spherical harmonic expansion is used for describing the field. The coefficients are derived under the assumption that the field can be represented by a scalar potential. This implies that measurements are made in a current free space. On ground and within the isolating atmosphere this is fulfilled. Nowadays global field models are based primarily on satellite observations. Dedicated magnetic field satellites are flying in the ionosphere. The question is, does this assumption also hold for them? Here we will give a short assessment of the currents in the night side ionosphere.

Charged particles are known to gyrate about the magnetic field. This circular motion generates a small additional magnetic field which has a direction opposite to the background field. The magnetic moment, M, comprising the product of the encircled area and the current strength can be written as

$$M = \pi R_g^2 \, \mathrm{I} \qquad (1)$$

where R_g is the gyro radius and I the current due to the moving charge. When inserting the relevant relations for these two quantities, we obtain the simple relation

$$M = \frac{kT}{B} \qquad (2)$$

where k is the Bolzmann constant, T the temperature and B the strength of the ambient magnetic field. It is worth nothing that the magnetic moment of a charged particle is neither depending on the mass nor on the charge state. M is also commonly called the *1st adiabatic invariant*. All this means that the presents of charged particles always reduces the ambient field strength.

Based on the evaluation of CHAMP magnetic field data Lühr et al. (2003) showed that the so-called diamagnetic effect of charged particle is also relevant in the ionosphere. They argue that to first approximation the sum of plasma pressure and magnetic field pressure can be regarded as constant. Based on this assumption the depletion of the field strength can be estimated

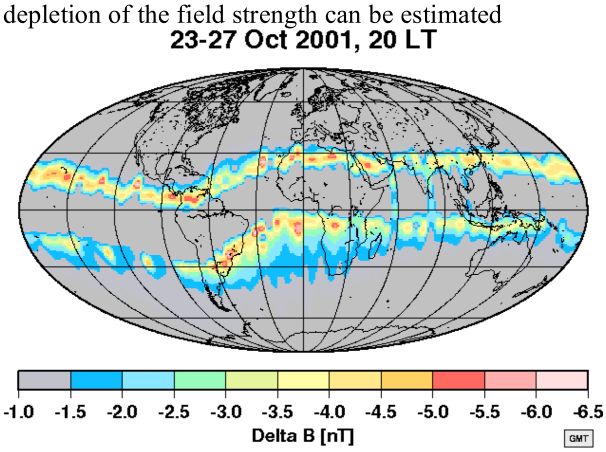

Figure 2. Diamagnetic effect of dense plasmas at 400 km altitude. Deficits in field strength of several nT are observed along the crests of the equatorial ionization anomaly (from Lühr et al., 2003).

$$\Delta B = \mu_o \, n \, k \left(T_i + T_e\right) / \, B \qquad (3)$$

where n is the electron density, T_i and T_e are the ion and electron temperatures. When applying measured plasma data to (3) the depletion in magnetic field can be estimated. Figure 2 shows as an average over 5 days the global distribution of the diamagnetic effect in the 20 LT sector. Outstanding are the two bands bracketing the magnetic dip equator. These coincide with the plasma enhancements in the Appleton anomaly. Even two hours after sunset the diamagnetic effect still amounts to -5 nT locally. Since the diamagnetic effect produces a systematic feature on the Earth's surface, these structures will directly enter magnetic field models if not corrected for. Only after midnight the plasma density has decayed below significance at 400 km altitude.

Another phenomenon which has to be mentioned in this context is ionospheric plasma instability. During the hours shortly after sunset instabilities form at the bottom side F region at equatorial latitudes. These are caused by steep upward directed plasma gradients (Whalen, 2000). At low altitudes the recombination rate is much faster than higher up. A small disturbance on the bottom-side can cause a local turn-over of this instable layering. In that case bubbles of depleted plasma, also calls equatorial spread-F (ESF), move upward. This phenomenon is also associated with the Appleton ionisation anomaly.

Figure 3 shows an example of magnetic field and plasma measurements, where CHAMP is passing through such plasma bubbles both in the northern and southern hemisphere. Concurrently with plasma density depletions, clearly visible in the bottom panel curve, enhancements in magnetic field strength occur (third panel from top). Also in the transverse components

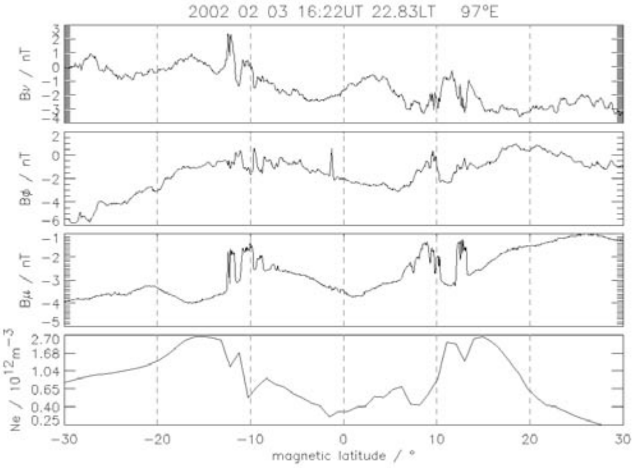

Figure 3. Magnetic and plasma density signature of plasma bubbles. Concurrent with the depletion in plasma density enhancements in the field strength occur. The magnetic field is presented in Mean-Field-Aligned coordinates. The third component is aligned with the main field, the second is perpendicular to the magnetic meridian, pointing eastward and the first completes the triad pointing outward. (from Stolle et al., 2006).

(upper two curves) associated variations are observed. While the enhanced field strength inside the bubbles compensate for the missing plasma pressure in the depleted flux tubes, can the transverse variations be regarded as indications for field-aligned currents.

A detailed investigation of the magnetic signatures associated with the plasma bubbles is performed by Stolle et al. (2006). In their statistical study they showed that the occurrence rate is high within the local time sector 19 – 24 LT. After mid night it rapidly decays off. Furthermore, the occurrence frequency exhibits a distinct seasonal, longitudinal distribution. Particularly outstanding is the high probability in the South America, Atlantic sector around December solstice. The authors furthermore found a linear dependence of the bubble occurrence rate on the solar EUV index, F10.7. This indicates that instable regions are encountered 4 to 5 times more frequently during solar maximum years compared to solar minimum. Interesting to note, there was no clear dependence on the magnetic activity index, K_p, observed.

Inside these rather localised flux tubes of depleted plasma the magnetic field strength is systematically enhanced by several nT. If not corrected for, it will cause spurious coefficients in main field models. But due to the small scale sizes of these structures a proper correction of the field modifications is rather difficult. It is therefore recommended to omit these parts of the orbit, which are affected, from magnetic model efforts. In particular, in case of constellation missions, such as

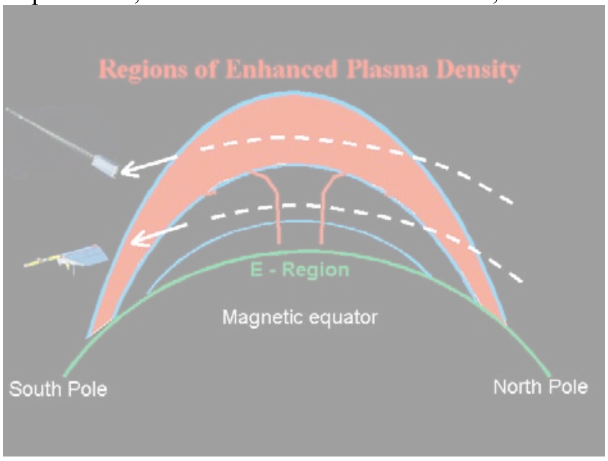

Figure 4. Sketch of satellite passes through the flux tube of the Equatorial Ionization Anomaly during the post-sunset hours. CHAMP is cruising at an altitude of about 400 km and Ørsted at 800 km.

Swarm, localized field modifications can cause large errors in the inter-satellite gradients.

Recently, another type of currents has been identified making significant contributions to magnetic field measurements on the night side. Due to the gravitational force ions experience a small eastward drift at equatorial and low latitudes. Electrons, due to their much smaller mass, are virtually unaffected. This differential motion sets up an eastward current, which is sometimes called the “ionospheric ring current”. Maximum current densities are found slightly above the peak of ionospheric F layer.

First experimental evidence for the gravity-driven currents was derived from CHAMP and Ørsted measurements. Particularly clear signatures could be found during the hours after sunset. During that time the ionospheric F region is lifted up by several hundred km at low latitudes. The Ørsted satellite with a mean altitude of about 800 km crosses approximately the centre of the current sheet near the equator. While CHAMP at a height of about 400 km stays below it at low latitude. The post-sunset plasma distribution and the orbital tracks of Ørsted and CHAMP are sketched in Figure 4. An eastward current generates a northward directed field below and a southward above the current sheet. This means, the geomagnetic field is enhanced below it and reduced above. When looking at satellite magnetic field residuals, which have been corrected for main field and magnetospheric field contributions, we find the expected signatures. The upper part of Figure 5 shows a comparison of field magnitude readings from Ørsted and CHAMP obtained within the local time sector 20 – 22 LT. Around the equator CHAMP detects an enhancement of the field strength by 3 – 4 nT, while Ørsted detects little variation in this latitude range. This

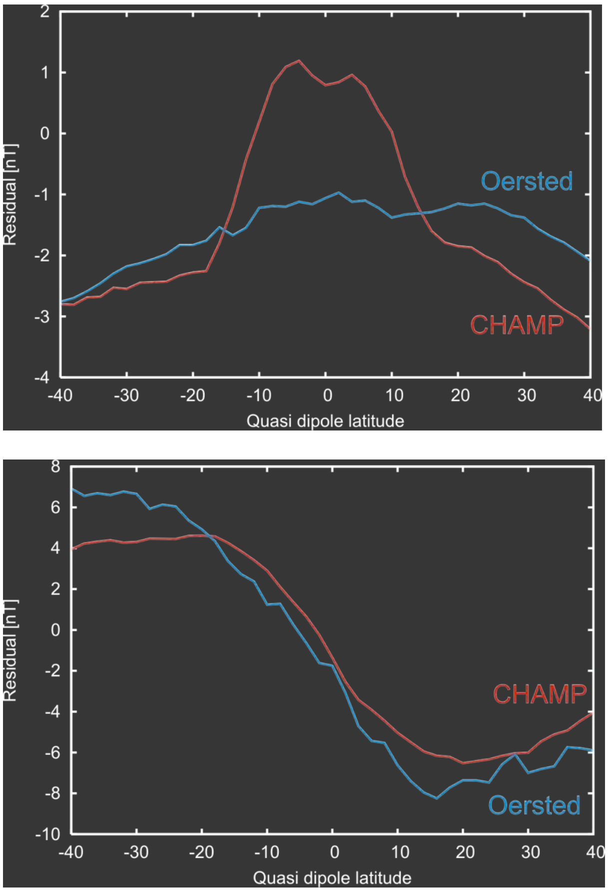

Figure 5. Magnetic signatures of gravity-driven currents at two altitudes during the post-sunset hours. (top panel) Residual of the field magnitude. Below the current the geomagnetic field is enhanced, at the center there is no influence. (bottom panel) Signature of the vertical magnetic field. This component varies slowly along a radial profile.

is the expected notation for passing below and through the current centre, respectively.

For completion, the lower part of Figure 5 shows the latitude variation of the vertical field component at the two altitudes. Both spacecraft record virtually the same field signature. This is expected since the vertical component exhibits an altitude profile which varies little through the current centre. From the slope of the curve at the zero-crossing the height-integrated current density can be estimated. It amounts to 7 mA/m. Likewise, the achieved amplitude, ±6 nT, give an indication of the total current strength (~50 kA).

A more rigorous treatment of the gravity-driven current in the Earth's ionosphere, as observed by CHAMP, has been given by Maus and Lühr (2006). They point out that proper treatments of the gravity-driven currents require knowledge of the ion density in the entire ionosphere. It is well-known that there is a higher electron density on the dayside than on the night side. In order to satisfy the current continuity requirement part of the dayside gravity-driven current has probably to be diverted from the equatorial F region along field lines near the evening terminator to the mid-latitude E region and routed back on that level to the morning side. For a full understanding of the current system a global modelling of the electrodynamics in the ionosphere would be required. Such a code has to consider all the relevant current contributions

$$\vec{j} = \underline{\underline{\sigma}}\left(\vec{E} + \vec{U} \, x \, \vec{B}\right) + \left[n m_i \, \vec{g} \, x \, \vec{B} - k\nabla\left\{(T_i + T_e)n\right\} x \, \vec{B}\right] \frac{1}{B?} \quad (4)$$

where $\underline{\underline{\sigma}}$ is the conductivity tensor, $\vec{E}$ the electric field, $\vec{U}$ the wind velocity, m_i the ion mass, $\vec{g}$ the gravitational acceleration, k the Boltzmann constant, T_i and T_e are the ion and electron temperatures. The first term in Eq. (4) represents the E-field-driven currents, the second gravity-driven and the third pressure-gradient-driven currents. Only the current contribution from the first term requires a formal conductivity. The other two can flow both on the day and on the night side. Since both latter terms scale with the electron density, their magnetic effect will be strongest in the F region. This is the height range at which the Swarm spacecraft are expected to fly.

So far we have focused on night side ionospheric currents. It has been demonstrated by Olsen et al. (2005b) that even current systems on the dayside can influence night time measurements. For example, the solar quiet, S_q, current system, driven by tidal winds on the dayside, also induces electric currents in the conducting Earth's mantle. At night, when the S_q currents are faded away, induced currents are still flowing, these cause, according to Olsen et al. (2005b), a bi-polar field in the radial direction with about 5 nT upward in the northern hemisphere and 5 nT downward in the southern. If not accounted for, these currents affect predominantly the Gauss coefficient g_3^0 in the main field model.

It has been shown in this section that there are several types of ionospheric currents that affect the magnetic field measurements on the night side. This is valid, in particular, for satellite measurements. In all the cases the magnetic effects were of the order of 5 nT. This is much larger than the envisaged accuracy of the Swarm magnetic field measurements. A more detailed investigation of the relevant current systems and a proper modelling of their effects is required, in order to design appropriate correction approaches. The high resolution of the foreseen instruments can only be fully exploited if the external fields are accounted for properly.

4. MAGNETIC FORCING OF THE THERMOSPHERE

The thermosphere, as the top layer of the atmosphere is characterised by a large variability in density and temperature in response to enhanced solar extreme ultraviolet (EUV) radiation and to geomagnetic disturbances. The morphology of these variations are rather complicated and so far not well described. This is to a good part due to a lack of well distributed, high-resolution neutral gas observations. This deficit is quite obvious in many cases when comparing actual measurements with predictions from atmospheric models like MSIS.

The situation has improved recently. Satellites like CHAMP and GRACE carry high-resolution accelerometers. From the experienced air drag the mass density can be derived. The obtained resolution in air density is better than $1 \cdot 10^{-14}$ kg/m³ at a sample rate of 0.1 Hz. On its near-polar orbit CHAMP circles the Earth more than 15 times per day since July 15, 2000. This long and continuous data record, covering all local times, allows studying a number of details in the upper atmosphere.

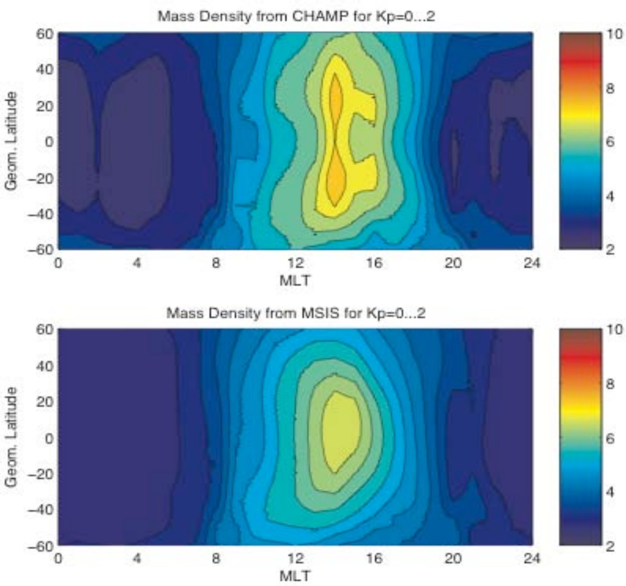

Figure 6. Diurnal variation of the total mass density as observed by CHAMP and as predicted by MSIS during quiet days. Of particular interest are the observed noon-time density maxima at mid-latitudes.

The basic equation for deriving the thermospheric density from acceleration measurements, $\vec{a}$, reads

$$\vec{a} = \frac{1}{2m} C_d \; \rho \; A_{eff} \; V^2 \; \vec{v} \qquad (5)$$

where m is the mass of the satellite, C_d the drag coefficient, ρ the mass density and A_{eff} the effective area in ram direction, which depends on the shape of the satellite and its orientation with respect to the flight direction. V is the total velocity with respect to the air at rest and $\vec{v}$ is the velocity unit vector in ram direction. The quantities m and C_d are known from the satellite design; A_{eff} and V can be derived from the orbit and attitude data. When inserting all these quantities into Eq. (5), the density, ρ, can be calculated straight forwardly.

In a statistical study Liu et al. (2005) have determined the diurnal distribution of average thermospheric density at 400 km altitude. One of the surprising features they have found is that the data are better organised in geomagnetic coordinates than in geographic. Figure 6 shows the average diurnal air density distribution for mid and low latitudes, both as measured and as predicted by the MSIS model. There is a general agreement between both panels, high densities at day time, low densities during the night. In detail there are subtle differences. Highest densities are not observed at the sub-solar point, as expected, but at mid latitudes. These mid latitude enhancements are recognisable until sunset. Nothing like that is reflected in the model prediction. This double hump in density resembles in some way the Equatorial Ionisation Anomaly (EIA). Liu et al. (2005) suggest that the anomalous density enhancements are caused by recombination of ions from the EIA. This process is associated with a release of energy. Since the ion dynamics is guided by the geomagnetic field, the feedback on the neutral atmosphere therefore also reflects the field geometry.

Characteristics at high latitude were also investigated by Liu et al. (2005). As an example, Figure 7 shows the relative difference between the observed air density and the predicted by MSIS. In both hemispheres there is a clear excess of density observed by CHAMP at high latitudes around the noon sector. This location coincides rather well with the ionospheric footprint of the magnetospheric cusp. Already Lühr et al. (2004) had reported distinct density enhancements in the cusp region. They related this thermospheric up-welling to Joule heating fuelled by small-scale field-aligned currents. This hypothesis was further investigated in a dedicated CHAMP-EISCAT measurement campaign (Schlegel et al., 2005). The previous results could be confirmed, but no conclusive answer for the heating mechanism was given. Further dedicated measurements are needed to explain this phenomenon.

Figure 7 also shows density enhancements around the midnight sector. These may be associated with sub-storm onsets. Intense upward field-aligned currents are accompanying the break-up manifesting themselves as westward travelling surges. The FACs are believed to carry the energy into the ionosphere. There are,

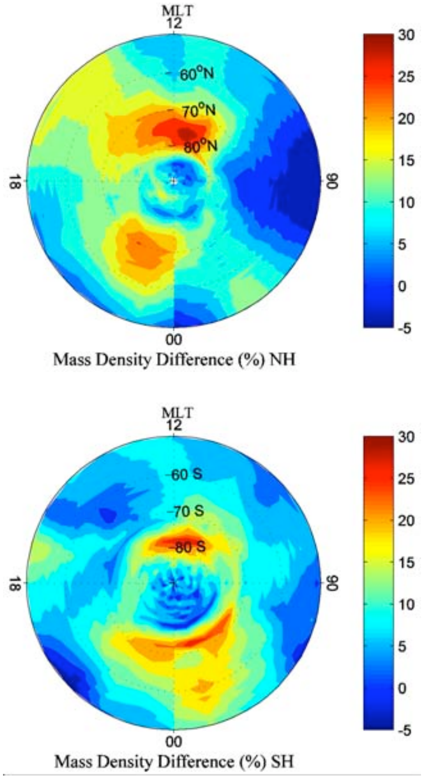

Figure 7. Percentage difference of the thermospheric density between CHAMP and MSIS90 in the polar regions for quiet conditions (from Liu et al., 2005).

however, no detailed studies so far investigating the relation between substorm onset and density enhancement on an event base.

In this section we have shown that there are several features of the thermosphere which are not captured by the models. They are generally related to the forcing of the neutral atmosphere by the geomagnetic field. Significant progress in the understanding of the thermosphere can only be achieved if simultaneous measurements of the neutral air dynamics are paired with high resolution magnetic field, as well as plasma and E-field observations.

5. CONCLUSIONS

In the sections above the important role was shown that the external fields play for the achievement of high-resolution main field models. New modeling approaches of the magnetospheric fields promise much better results both for the main field and ionospheric current studies.

A whole variety of newly identified ionospheric currents systems at F region heights has been described. These currents are active both at night and day. Since the Swarm satellites will fly at that altitude, an effective removal of the disturbances is required before the magnetic field measurements can be interpreted as potential fields. The E-field and plasma instruments are required to achieve that goal.

The thermospheric density and winds are intimately coupled to the ion dynamics. Therefore the geomagnetic field, as a guiding system, plays a major role in controlling the location of the coupling processes. Only when neutral gas dynamics is observed together with the plasma parameters and the magnetic field progress in the high atmosphere research can be made. The Swarm mission promises to provide the right tools.

REFERENCES

1. Campbell, W.H., An external current representation of the quiet night-side geomagnetic field level changes, *J. Geomag. Geoelectr.,* **36,** 257-265, 1984.
2. Langel, R.A. and R.H. Estes, Large-scale,near-Earth magnetic fields from external sources and the corresponding induced internal field, *J. Geophys. Res.,* **90,** 2487-2494, 1985.
3. Langel, R.A., T.J. Sabaka, R.T. Baldwin, and J.A. Conrad, The near-Earth magnetic field from magnetospheric and quiet-day ionospheric sources and how it is modelled, *Phys. Earth Planet. Int.,* **98,** 235-267, 1996.
4. Liu, H., H. Lühr, V. Henize and W. Köhler, Global distribution of the thermospheric total mass density derived from CHAMP, *J. Geophys. Res.,* **110,** A04301; doi:10.1029/2004JA010741, 2005.
5. Lühr, H., M. Rother, S. Maus, W. Mai, and D. Cooke, The diamagnetic effect of the equatorial Appleton anomaly: Its characteristics and impact on geomagnetic field modelling, *Geophys. Res. Lett.,* **30**(17), 1906, doi: 10.1029/2003GL017407, 2003.
6. Lühr, H., M. Rother, W. Köhler, P. Ritter, L. Grunwaldt, Thermospheric up-welling in the cusp region, evidence from CHAMP observations, *Geophys. Res. Lett.,* **31,** L06805, doi:10.1029/2003GL019314, 2004.
7. Maus, S. And P. Weidelt, Separating the magnetospheric disturbance magnetic field into external and transient internal contributions using a 1D conductivity model of the Earth, *Geophys. Res. Lett.,* **31,** L12614, doi:10.1029/2004GL020232, 2004.
8. Maus, S., H. Lühr, G. Balasis, M. Rother and M. Mandea, Introducing POMME, The Potsdam Magnetic Model of the Earth, in *Earth Observation with CHAMP, Results from Three Years in Space,* (eds.) C. Reigber, H. Lühr, P. Schwintzer and J. Wickert, pp. 293-298, Springer, Berlin – Heidelberg, 2005.
9. Maus, S. and H. Lühr, Signature of the quiet-time magnetospheric magnetic field and its

electromagnetic induction, *Geophys. J. Int.,* doi:10:1111/j.1365-246X.2005.02691.x, 2005.
10. Maus, S. and H. Lühr, A gravity-driven electric current in the Earth's ionosphere identified in CHAMP satellite magnetic measurements, *Geophys. Res. Lett.,* **33,** L02812, doi:10.1029/2005GL024436, 2006.
11. Olsen, N., A model of the geomagnetic main field and its secular variation for epoch 2000 estimated from Ørsted data, *Geophys. J. Int.,* **149,** 454-462, 2002.
12. Olsen, N., T.J. Sabaka, and F. Lowes, New parameterization of external and induced fields in geomagnetic field modelling, and a candidate model for IGRF 2005, *Earth Planet Space,* **57,** 1141-1149, 2005a.
13. Olsen, N., F. Lowes, and T.J. Sabaka, Ionospheric and induced field leakage in geomagnetic field models, and derivation of candidate models for DGRF 1995 and DGRF 2000, *Earth Planet Space,* **57,** 1191-1196, 2005b.
14. Schlegel, K., H. Lühr, J.-P. St.-Maurice, G. Crowley, and C. Hackert, Thermospheric density structure over the polar regions observed with CHAMP, *Ann. Geophys.,* **23,** 1659-1672, 2005.
15. Stolle, C., H. Lühr, M. Rother, and G. Balasis, Magnetic signatures of equatorial spead-F, as observed by the CHAMP satellite, *J. Geophys. Res.,* **111,** A02304, doi:10.1029/2005JA011184, 2006.
16. Utada, H., T. Koyama, H. Shimizu and A.D. Chave, A semi-global reference model for electric conductivity in the mid-mantle beneath the north Pacific region, *Geophys. Res. Lett.,* **30,** 43-1, dio: 10.1029/2002GL016092,2003.
17. Whalen, J.A., An equatorial bubble: Its evolution observed in relation to bottomside spread-F and the Appleton anomaly, *J. Geophys. Res.,* **105,** 5303-5315, 2000.